Research Article 2017, **2**(1) 61-66 Advanced Materials Proceedings

H_2 and CO gas sensor from SnO_2/polyaniline composite nanofibers fabricated by electrospinning

Hemlata J. Sharma*, Megha A. Salorkar, Subhash B. Kondawar

Department of Physics, Rashtrasant Tukadoji Maharaj Nagpur University, Nagpur 440033, India

*Corresponding author, Tel: (+91) 71-22042086; E-mail: sbkondawar@yahoo.co.in

Received: 31 March 2016, Revised: 26 September 2016 and Accepted: 30 November 2016

DOI: 10.5185/amp.2017/114
www.vbripress.com/amp

Abstract

Electrospun nanofibers of Polyaniline (PANI)/SnO_2 composite based gas sensor for hydrogen (H_2) and carbon monoxide (CO) gas were prepared by electrospinning technique. The synthesized material was characterized using UV-Visible, XRD and SEM-EDX analyses. The average diameter of PANI/SnO_2 composite was found to be high as compared to that of pristine SnO_2 nanofibers having 200 nm diameter may be due to micelle formation of PANI on the surface of SnO_2 nanofibers. The enhanced sensing properties in the form of sensitivity factor, time taken to response and recovery during exposure and de-exposure of Gas and repeatability were studied. The SnO_2/PANI composite nanofibers showed high sensitivity and response to H_2 gas compared to CO gas to 0.1% and maximum sensitivity was observed at 35˚C for H_2 gas. Fast Response-Recovery Time for 1000-5000 ppm of H_2 i.e. less than 30 secs were observed. Due to room temperature operation of the sensor, it is promising for environmental applications. The results indicate that aligned SnO_2/PANI composite fibers are promising candidate for fast detection of H_2 gas. Copyright © 2017 VBRI Press.

Keywords: Nanofibers, polyaniline/SnO_2, nanocomposites, electrospinning, gas sensing.

Introduction

Today gas sensors are highly in demand for detecting, monitoring and controlling the presence of hazardous and poisonous gases into the atmosphere. Sensors working at low operating temperature have received excellent attention due to its environmental monitoring and health related problems. The electrical conductivity of the sensor changes upon exposure to particular gas is used for the detection of any toxic gas. There are several important factors for the gas sensor such as sensitivity, selectivity, stability, reproducibility, response-time and recovery-time. Some gases are so much hazardous that they cannot be detected by human senses. So, to detect and monitor the gases accurately, gas sensors are required which would work at room temperature. However, highly sensitive hydrogen and carbon monoxide detection is essential for early leakage warnings and prevention of explosion at room temperature. Carbon monoxide (CO) and hydrogen (H_2) are dangerous gases on Earth's surface. By now, a great deal of work on H_2 and CO sensors has been reported **[1]**. Gas detectors can be used to detect combustible, flammable and toxic gases, and oxygen depletion. This type of device is used widely in industry and can be found in locations, such as on oil rigs, to monitor manufacture processes and emerging technologies such as photovoltaic. They may be used in firefighting. These sensors usually employ an audible alarm to alert people when a dangerous gas has been detected. Common sensors include infrared point sensors, ultrasonic sensors, electrochemical gas sensors, and semiconductor sensors. All of these sensors are used for a wide range of applications and can be found in industrial plants, refineries, waste-water treatment facilities, vehicles, and homes. Semiconductor sensors detect gases by a chemical reaction that takes place when the gas comes in direct contact with the sensor. Nanofibers based sensors possess enhanced sensing properties such as small diameter, high aspect ratio and so on. In addition, they have very large specific surface area which can be helpful to improve the sensing properties due to the larger exposure of functional materials. Semiconducting metal-oxide nanofibers have been successfully fabricated and widely utilized for gas sensors due to their sensing properties based on the surface reaction between the metal-oxides and adsorbed gas species on exposure to specific gas. Semiconducting nanomaterials (ZnO, SnO_2, TiO_2, WO_3, In_2O_3 etc.) have shown excellent sensing properties **[2-4].** Among the metal oxide, pure tin oxide, SnO_2 is an excellent sensing material and has good sensing results at very high operating temperature as shown in literature survey for the detection of various reducing and oxidizing gases. Gas interaction in SnO_2 is done by the reaction and adsorption of oxygen on its surface. Also, the nanofibers of pristine SnO_2 have been exposed with high sensing characteristics, by showing the change in conductivity but the high operating temperature (200-400˚C) of these sensors may be inadequate for measuring high gas concentrations due to the danger of explosions. So, much focus has been done to develop the gas sensor works at low operating temperature and require low power to consume. Organic conducting polymers are the new kind of materials which help us to work at room temperature and have controllable conductivity and environmental stability which is advantageous over metal oxide based sensors because they need several hundred-degree celsius temperature to operate. These conducting polymers also help to enhance sensing characteristics by several orders of magnitude, stability, selectivity, sensitivity, reproducibility, response -recovery behavior, and several other properties. So, gas sensing properties could be improved at room temperature by using conducting polymers. As we have discussed, use of these conducting polymers enhances the sensitivity, reproducibility, solubility and selectivity of the sample **[5-9]**. Among various conducting polymers, PANI is an excellent semiconducting polymer and has large number of properties and applications. It has controllable electrical conductivity, good environmental stability and has interesting redox properties. It is excellently used as a sensing material because it has an ability to form composites and produce synergetic effects even at room temperature. Due to these characteristics, we are using this polymer not only in sensing but also in various fields, electromagnetic shielding, anti-corrosion, and tissue engineering etc. There is a tremendous approach for the enhancement of the mechanical strength and characteristics of sensors by combining the organic materials with inorganic counterparts to form composites. Because pure polyaniline has poor sensitivity and also it has very poor solubility in organic solvents as compared to tin-oxide so it can’t be used alone as a gas sensor. And it is unsuitable as a gas sensor individually. By adding nanostructure SnO_2 into PANI matrix can improve the sensitivity of composites due to the synergistic effect and also overcome the limitations based on pure PANI, nanocomposites have been investigated as the suitable gas sensing materials **[10-11]**. The synergistic effect of composite can be seen by combining organic and inorganic material individually and PANI/SnO_2 composite had excellent gas sensing properties **[12-13]**. The nanofibers of polymeric materials have large aspect ratio, large surface area to volume ratio and large porosity, such materials are best for sensing of different gases due to larger absorptive capacity for gas analyte. The porous microstructure and surface reactivity are key parameters for the performance of nanofibers based sensor **[14]**. These sensors have large pore volume, suitable pore size, its distribution and large surface area has high sensitivity. There are different methods used to fabricate PANI nanofibers include hard templates, soft templates **[15]**, seeding, interfacial polymerization, rapidly mixing **[16],** and electrospinning **[17, 18]**. Among these techniques, we have chosen electrospinning, for the production of fibers with diameter in nanoscale regime. Electrospinning is a simple technique to produce polymer nanofibers by accelerating high voltage power supply to the polymer solution. Fibers produced by this technique have very high surface area to volume ratio, highly porous structure, high aspect ratio and diameter around tens to hundreds of nanometers. They have conductivity with uniform structure. Electrospinning technique has very low manufacturing cost and it is also mass production technique. It involves electro-spraying as well as spinning of fibers. High temperature operation is prohibited here due to danger of explosions. So, there is no need to use high temperature for producing solid threads from spinning solution. There are several factors on which this technique works. The solution must have very high conductivity. So, that it could gain sufficient charges and the electrostatic repulsion of the solution counteracts the surface tension of the solution. The solution must be viscous. At very high voltage, the charges in the solution develops, and electrostatic repulsion counteracts the surface tension of solution and stretching of droplet takes place; at a particular voltage, a stream of liquid erupts from the surface. This is known as the Taylor cone. If the cohesion is high, then continuous jet of fibers is obtained on the collector. Due to the elongation and thinning of the fiber obtained from this bending instability, uniformity and porosity of fibers increases.

In this article, we report the fabrication of SnO_2/PANI composite nanofibers by electrospinning for H_2 and CO gas sensing properties at low temperature. The synthesized sample was characterized by various gas sensing parameters in terms of sensitivity, response time, recovery time and repeatability using a static gas sensing system for hydrogen and CO gas. Composite nanofibers showed good response-recovery with good reproducibility in comparison with pure SnO_2 and pure PANI nanofibers at room temperature. The composite nanofibers showed higher response towards hydrogen gas than CO gas.

Experimental

Materials/ chemicals details

Tin chloride ($SnCl_2$•$2H_2O$, purity 99%), Aniline monomer (distilled under reduced pressure) (purity 98.5%), ammonium peroxydisulphate (APS, purity 99%), Camphor sulfonic acid (CSA, purity 99%) and polyvinyl pyrrolidone (PVP, Mw=1,300,000, purity 99%) were purchased from Sigma-Aldrich. All other chemicals were used as received without any further purification.

Preparation of pure SnO_2 nanofibers

0.4 g of $SnCl_2 \cdot 2H_2O$ was mixed with DMF and ethanol, and then the mixture was magnetically stirred for 10 min. 1.0 g PVP was added into the above solution and solution was used as electrospinning precursor. The solution was then electrospunned and the fibers were collected on the aluminium foil. The synthesized sample was then calcined at 300˚C in air for 4 h to remove the organic constituents of PVP and to crystallize the SnO_2.

Preparation of SnO_2/PANI composite nanofibers

The SnO_2/PANI nanocomposite was prepared by chemical oxidative polymerization of aniline on the substrate bearing SnO_2 nanofibers. The concentration of both the dopant CSA and the oxidizing agent (APS) was 0.5 M and 0.2 M respectively, and the coated aniline was 0.2 M. SnO_2/PANI nanocomposites were fabricated by depositing a layer of PANI on the sensors based on SnO_2 nanosheets via simple dip-coating in the aqueous solution of water- processable PANI. Typically, the electrode with as-prepared SnO_2 nanosheets was dipped into an aqueous solution of 0.5 M camphor sulphonic acid (CSA) and 0.2 M ammonium peroxydisulphate (APS) using a home-made automatic dip-coating machine. The resulting electrode was dried in air, and put into a closed vacuum vessel which was evacuated with a vacuum pump. Then 0.2 M of aniline was injected, and vapor phase polymerization proceeded under reduced pressure for 24 h at room temperature (~20^{o}C). Subsequently, the electrode was rinsed with deionised water and dried in air, obtaining a gas sensor based on the composite of SnO_2 nanosheets and PANI doped with CSA. For comparison, gas sensors based on PANI alone were prepared with the electrodes free from SnO_2 nanosheets using the same methods. PVP nanofibrous template via electrospinning technique was prepared and then, deposition of PANI was done to get nanofibrous film of pure PANI.

Characterizations

Scanning Electron Microscopy (SEM) and Energy Dispersive X-ray spectroscopy (EDX) were done by Carl Zeiss EVO-18 model SEM-EDX. UV-Visible absorption spectrum was obtained by Shimadzu-UV-1800 spectrophotometer. X-ray diffraction (XRD) pattern was obtained by Philips-PW1710 automatic X-ray diffractometer. The gas sensing behaviour was studied using laboratory built up sensing apparatus by measuring change in the resistance of composite nanofibers with optimized operating temperature in the range of 30˚- 60˚C towards pure air, hydrogen and CO gas exposure. The resistance variation was measured by Keithley 2000 Multimeter and temperature was controlled by Temperature Controlled VI Characterization System. Different concentrations (1000-5000 ppm) of H_2 was obtained by diluting standard H_2 with dry compressed air using computer-driven digital mass flow controllers. The organic vapors of different concentrations were obtained by injecting a calculated quantity of organic liquid into a testing chamber filled with dry air and equipped with an electric fan.

Results and discussion

UV-VIS was carried out to study the conducting states in the samples corresponding to their absorption bands **[19-20]**. In **Fig. 1,** graph between absorbance and wavelength is shown for pure SnO_2 and tin oxide/PANI nanocomposite fibers. The three prominent absorption peaks in nanocomposite confirms the formation conducting polymer as well as metal oxide based composite material. Peak at ~304 nm, is for pure SnO_2; whereas in case of SnO_2/PANI nanocomposites, the peaks at ~304, ~405 and ~860 nm, respectively was observed. It is interesting to note that the characteristic peak of the pristine SnO_2 appear in the composite nanofibers. This indicates the presence of SnO_2 in synthesized composite sample. Peaks at 405 and 860 nm in visible region attributed to inter ring charge transfer ratio of benzenoid to quinoid units which shows polaron-π* and π-polaron transition respectively and peak at 304 nm in UV region attributed to π-π* transition of benzenoid unit and the insertion of SnO_2 in PANI **[20]**.

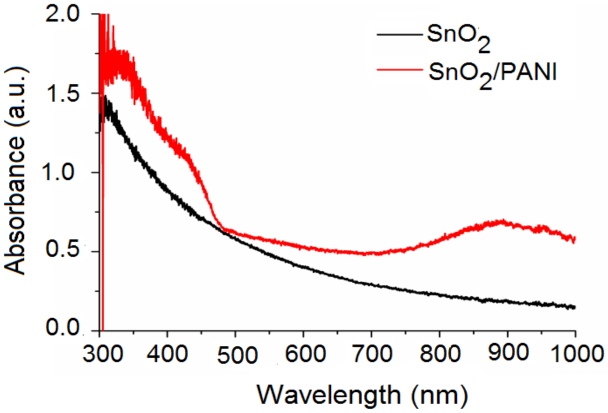

Fig. 1. UV-VIS spectra of nanofibers.

In **Fig. 2**, the crystal structure of SnO_2 and PANI/SnO_2 fibers was examined by X-ray diffraction (XRD). All polymer chain does not match identically due to the different chain structure **[21]**. All the strong diffraction peaks of SnO_2 can be perfectly indexed as the tetragonal rutile structure for SnO_2 (ICDD DATA CARD (41-1445) **[22]**. The broad amorphous peak in composite implied the existence of PANI. Some of the observed characteristic peaks for composite sample were well matched with the pure SnO_2 which clearly showed that the composite sample contains SnO_2 particles. The crystallization behaviour of pristine SnO_2 nanofibers was affected due to the formation of composite sample.

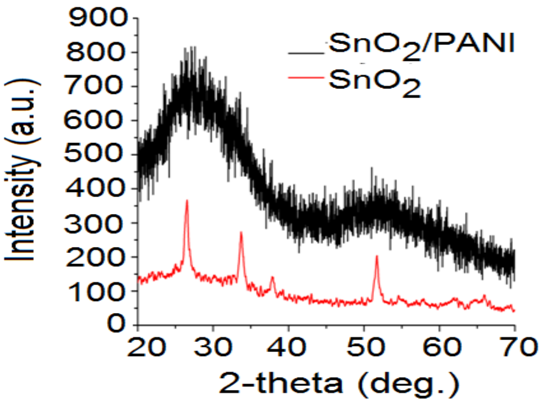

Fig. 2. XRD patterns of nanofibers.

SEM images for pure SnO_2 and composite nanofibers are shown in **Fig. 3** after calcinations at 300˚C of pure SnO_2 nanofibers. During the thermal treatment, PVP was removed. It is observed that diameter of pure sample was in the range of 100-200 nm and have uniformity in structure. The pristine SnO_2 nanofibers are uniformly encapsulated by the polymer and are not enclosed to the environment which could also help to enhance the sensing characteristic of composite pure nanofibers with crystallite sizes were about 10-15 nm and in composite, the diameter is slightly increased may be due to the encapsulation of PANI over pristine SnO_2. Due to the porous nature, random distribution of fibers can be seen. The diameter of pristine sample was somewhat less as compared with the composite sample but porosity was not there. So, it would not help us in improving our results. The composite fibers have well aligned structure and have highly porous structure. It indicates that the composite is good for gas sensing as compared to that of pure SnO_2.

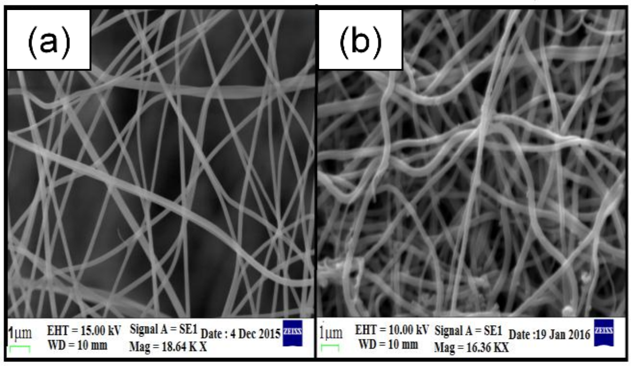

Fig. 3. SEM image (a) pure SnO_2 and (b) SnO_2/PANI nanofibers.

EDX has been used to investigate the compositions of the sample, and the spectra are illustrated in **Fig. 4**. Fibers had a polycrystalline nature which can be seen from the SEM images and confirmed by the crystalline peaks of XRD analysis. The Energy Dispersive X-Ray Spectroscopy (EDX) analysis confirmed that the samples (nanofibers) contain O, Sn, C and N atoms. The H signal in composite is not present due to its lower energy. The characteristics of the fibers (with multiple nanograins) and porosity of the obtained samples are features particularly useful for gas sensing applications where the surface plays an important role in the detection process.

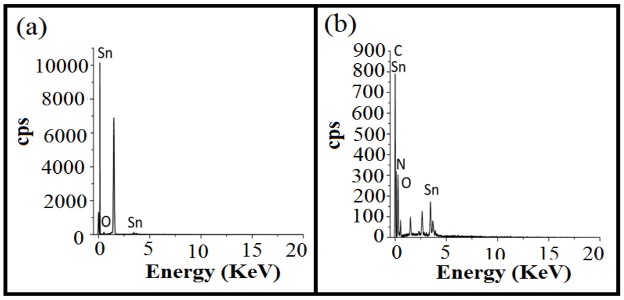

Fig. 4. EDX image (a) pure SnO_2 and (b) SnO_2/PANI nanofibers.

Fig. 5 shows the schematic diagram of gas sensing apparatus. It consists of two cylinders, one is of air and other is of H_2 gas connected to the gas chamber using three way stop-cock. Inside the chamber, temperature is maintained with the help of thermocouple (heater controller). There is a glass substrate, on which sample is mounted provided with electrode in order to detect change in resistance of material on exposure and de-exposure of gas. These electrodes connected to thermos-resistor (multimeter) which is operated via software so that output can be obtained on computer in the form of change in resistance of sensing material with respect to change in time and temperature which shows that electrical resistance is a sensitive parameter in case of sensing. Current –Voltage (I-V) characteristics of composite nanofibers were recorded at various concentration of gas on exposure and on removal of hydrogen gas. From this, we can calculate the resistance of sample R_a, Resistance in presence of air and R_g, Resistance in presence of gas molecules. By calculating resistance all sensing parameters can be easily calculated.

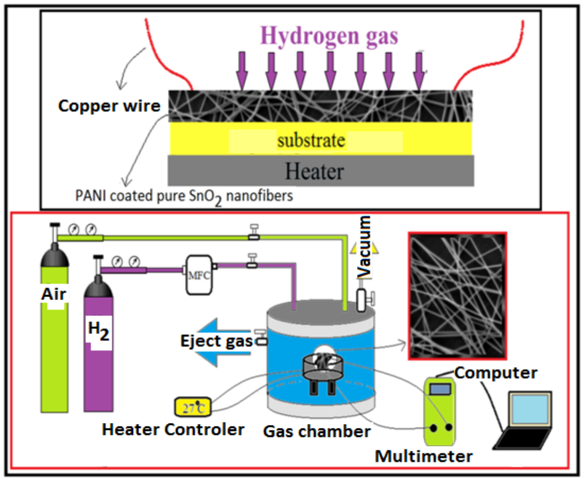

Fig. 5. Schematic diagram of hydrogen sensing apparatus.

First the sensor was stabilized for 6h before gas exposure. After resistance stabilization, gas was injected into the chamber. The composite sensor was then exposed with the hydrogen gas and sensitivity was recorded at various temperatures. After that response and recovery of the gas was also checked on exposure and removal of gas continuously to find out its reproducibility. During exposure of gas to the composite sample some chemical reactions takes place between sample and adsorbed gas species. These gas molecules reached to the depletion layer of composite on its gas exposure and reactions occurred at the surface of junction layer and due to hopping effects, change in conductivity of sample occurs and which is an important parameter in case of sensing of material.

PANI is a p-type material and SnO_2 is an n-type semiconducting material. So, heterojunction is formed between p-and n- type material and a junction layer is formed between them. When hydrogen gas comes in contact with the junction layer of composite material, its resistance changes, due to the structural modification of synthesized composite sample electronically **[23]**. This junction layer plays a very important role in case of sensing and to enhance the conductivity of sample on gas exposure. As hydrogen is a reducing agent, so it increases the conductivity of the sample on gas exposure. The gas sensing mechanism of PANI based sensors occurs due to the reaction between its surface and H_2 gas. According to this mechanism it is possible that, gas molecules react with nitrogen atoms at imine sites of doped PANI and these hydrogen molecules might form a bridge between nitrogen atoms of two polymer chains. Thus, dissociation of H_2 bonds takes place and new N-H bonds formed in the polymer chain. Due to which the hopping conductivity of chain increases thereby, creates polaronic lattice sites (a combination of charge and the chain deformation) with a redistribution of polaron energy density in the forbidden energy gap that causing new charge transport features create. The numbers of charge particles increase which would help to increase the rate of charge transfer in presence of gas molecules in inter polymer chain and could help to reduce the resistivity of sample and enhance the conductivity of composite **[24-25]**. It is found that the nanocomposite exhibits Ʈ$_{response}$ and Ʈ$_{recovery}$ (which is defined as the time to reach 90% of the resistance change during exposure and on removal of gas resp.). The values of Ʈ$_{response}$ and Ʈ$_{recovery}$ were found to be < 30 sec. From literature survey, available in this regard, we found that pure SnO_2 based sensors available in the market doesn't show any change in its resistance at room temperature. Even when high concentration of gas exposure, SnO_2 films remained insensitive at room temperature because they need very high temperature to operate. However, SnO_2/Polyaniline composite film showed appreciable sensitivity for 1000-5000 ppm of H_2 gas. Maximum sensitivity of composite was observed at 35˚C on exposure to different concentrations of H_2 gas. It is observed that the response of the sensor increases first as we increase the temperature and then again decrease as we increase the temperature further and due to which we get optimal operating temperature of the sensor *i.e.* 35 ˚C.

The polyaniline-SnO_2 composite nanofibers showed a very high sensitivity to H_2 gas at room temperature as compared to CO gas at 1000 ppm which is constant throughout all temperatures shown in **Fig. 6(a)** and as the concentration of H_2 gas increases then sensitivity increases rapidly, as shown in **Fig. 6(b) [26-34]**. **Fig. 6(c)** shows the Response-Recovery Time graph for 1000-5000 ppm of H_2 gas at 35˚C. Further, the measurement of gas sensing properties of composite film for number of cycles at various ppm concentration of hydrogen gas clearly indicate the repeatability of gas sensing response of the film.

Conclusion

Electrospinning technique followed by chemical oxidative polymerization method was used to fabricate SnO_2/PANI composite nanofibers based gas sensor. The formation of this composite sample was confirmed from UV-vis, XRD and SEM-EDX characterizations. The SEM images showed the formation of nanofibers with diameter in nanoscale regime. The SnO_2/PANI composite nanofibers

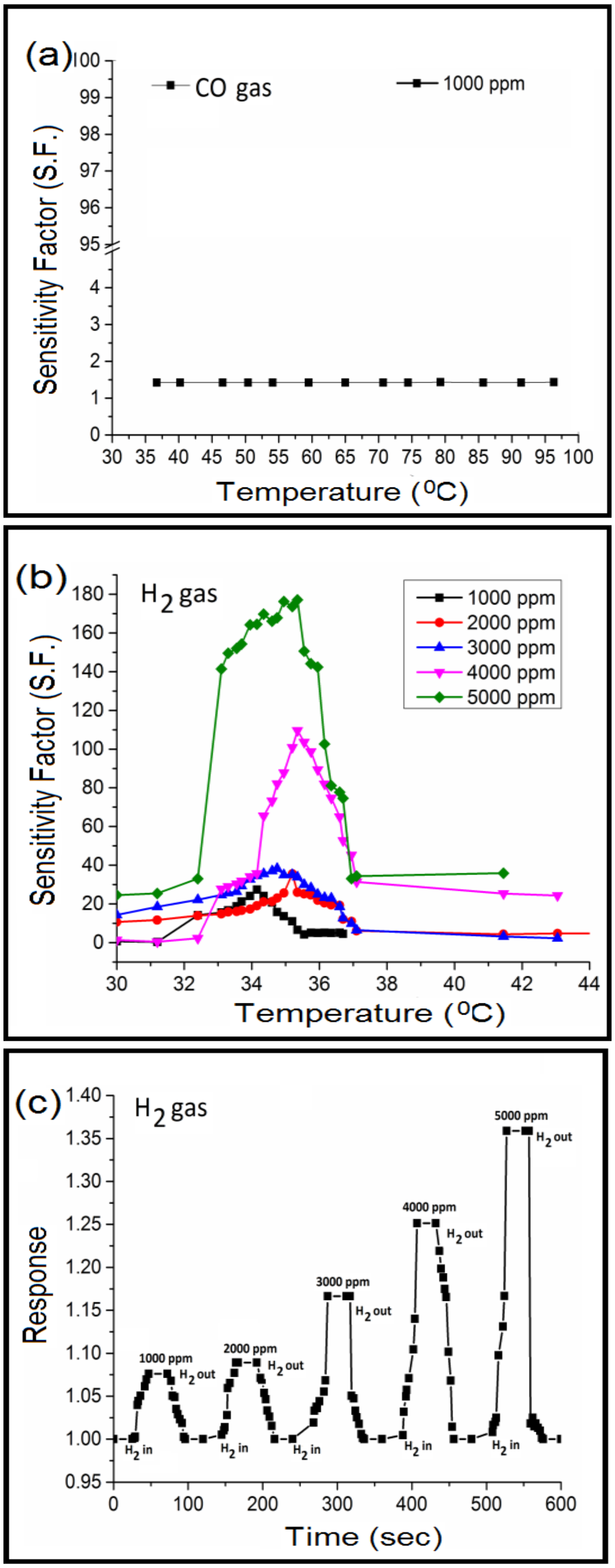

Fig. 6. (a) Sensitivity of CO gas (b) Sensitivity of H_2 gas (c) Response-Time graph of SnO_2/PANI composite nanofibers.

showed high sensitivity to H_2 gas compared to CO gas at 1000 ppm and as the concentration of H_2 gas increases then sensitivity increases rapidly and maximum sensitivity was observed at 35˚C for H_2 gas. Response-Recovery Time for 1000-5000 ppm of H_2 gas was found to be < 30 sec. The proposed sensing mechanism was related to the existence of p-n heterojunction in the SnO_2/PANI hybrid material. Hence, the synthesized sample used as a gas sensor has the potential to work for environmental monitoring.

Acknowledgements

This work is supported by Department of Science & Technology, New Delhi (India) under INSPIRE Fellowship (No. DST/INSPIRE Fellowship/ 2013/92, IF130149 for financial assistance.

Author's contributions

Conceived the plan: S.C., S.C*; Performed the experiments: C.D.; Data analysis: S.C., S.C*, A.K; Wrote the paper: S.C., S.C*., C.D. Authors have no competing financial interests.

References

1. Rad, A.; Nasimi, N.; Jafari, M.; Shabestari, D.; Gerami, E.; *Sens. Actuators, B*, **2015**, *220*, 641. **DOI:** 10.1016/j.snb.2015.06.019
2. Deshpande, N.; Gudage,Y.; Sharma, R.; Vyas, J.; Kim, J.; Lee, Y.; *Sens. Actuators, B*, **2009**, *138*, 76. **DOI:** 10.1016/j.snb.2009.02.012
3. Tiwari, A.; Gong, S.; *Electroanalysis*, **2008**, 20, 1775.
4. Sharma, H.; Sonwane, N.; Kondawar, S.; *Fibers Polym.*, **2015**, *16*, 1527. **DOI:** 10.1016/j.mspro.2015.06.040
5. Kim, B.; Oh, S.; Han, M.; Im, S.; *Synth. Met.*, **2001**, *122*, 297. **DOI:** 10.1016/S0379-6779(00)00304-0
6. MacDiarmid, A.; Epstein. A.; *Synth. Met.*, **1994**, *65*, 103. **DOI:** 10.1016/0379-6779(94)90171-6
7. Monredon, S.; Cellot, A.; Ribot, F.; Sanchez, C.; Armelao, L.; Gueneau, L.; Delattre, L.; *Mater.Chem.*, **2002**, *12*, 2396. **DOI:** 10.1039/B203049G
8. Kondawar, S.; Agrawal,S.; Nimkar, S.; Sharma,H.; Patil, P.; *Adv. Mater. Lett.*, **2012**, *3*, 393. **DOI:** 10.5185/amlett.2012.6361
9. Kondawar, S.; Acharya, S.; Dhakate, S.; *Adv. Mater. Lett.*, **2011**, *2*, 362. **DOI:** 10.5185/amlett.2011.9107am2011
10. Wankhede,Y,; Kondawar,S.; Thakare, S.; More, P.; *Adv. Mater. Lett.*, **2013**, *4*, 89. **DOI:** 10.5185/amlett.2012.icnano.108
11. Nandapure, B.; Kondawar, S.; Salunkhe, M,; Nandapure, A.; *Adv. Mater. Lett.*, **2013**, *4*, 134. **DOI:** 10.5185/amlett.2012.5348
12. Kondawar, S.; Patil, P.; Agrawal, S.; *Adv. Mater. Lett.*, **2014**, *5*, 389. **DOI:** 10.5185/amlett.2014.amwc.1037
13. Chen, J.; Yang, J.; Yan, X.; Xue, Q.; *Synth. Met.*, **2010**, *160*, 2452. **DOI:** 10.1016/j.synthmet.2010.09.026
14. Kondawar, S.; Pethe, S.; *Adv. Mater. Lett.*, **2014**, *5*, 414. **DOI:** 10.5185/amlett.2014.amwc.1039
15. Grimm, S.; Giesa, R.; klarek, K.; Langner, A.; Gosele, U; Schmidt, H.; Steinhart, M.; *Nano Lett.*, **2008,** *8*, 1954. **DOI:** 10.1021/nl080842c
16. Guana, H.; Fana, L.; Zhanga, H.; Qua, X.; *Electrochim. Acta.*, **2010,** *56*, 964. **DOI:** 10.1016/j.electacta.2010.09.078
17. Huang, J.; *Pure Appl. Chem.*, **2006**, *78*, 15. **DOI:** 10.1351/pac200678010015
18. Tiwari, A.; Kobayashi, H. (Eds.); Responsive Materials and Methods; Wiley: USA, **2013**. **DOI**: 10.5185/sbm-2010-01
19. Tseng, R. J.; Huang, J.; Ouyang, J.; Kaner, R. B.; Yang, Y.; *Nano Lett.* **2005**, *5*, 1077. **DOI:** 10.1021/nl050587l
20. Jing, X.; Wang, Y.; Wu, D.; Qiang, J.; *Ultrason. Sonochem.*, **2007,** *14*, 75. **DOI:** 10.1016/j.ultsonch.2006.02.001
21. Olad, A.; Nosrati, P.; *Res. Chem. Intermed.*, **2012**, *38*, 323. **DOI:** 10.1007/s11164-011-0349-0
22. Yang, M.; Cao, K.; Sui, L.; Ying, Q.; Zhu, J.; Waas, A.; Arruda, E. M.; Kieffer, J.; Thouless, M. D.; Kotov, N. A.; *ACS Nano.*, **2011**, *5*, 6945. **DOI:** 10.1021/nn2014003
23. Chang, S.; Hsueh, T.; Chen, I.; Hsieh, S.; Chang, S.; Hsu, C.; Lin, Y.; Huang, B.; *IEEE Trans. Nanotechnol.*, **2008**, *7*, 754. **DOI:** 10.1109/TNANO.2008.2005917
24. Ali, Y.; Kumar, V.; Dhaliwal, A.S.; Sonkawade, R.G.; *Adv. Mat. Lett.*, **2013**, *4*, 368. **DOI:** 10.5185/amlett.2012.9422
25. Sanjay, S.; Yadav, R.; Pandey, A.; *Adv. Mat. Lett.*, **2013**, *4*, 378. **DOI:** 10.5185/amlett.2012.9427
26. Greiner, A.; Wendorff, J.; Angew; *Chem. Int. Ed.*, **2007,** *46*, 5670. **DOI:** 10.1002/anie.200604646
27. Wu, W.; Zhang, S.; Xiao, X.; Jiang, C.; *Adv. Mat. Lett.*, **2013**, *4*, 610. **DOI:** 10.5185/amlett.2012.12477
28. Mathai, C.; Saravanan, S.; Anantharaman, M.; Venkitachalam, S.; Jayalekshmi, S.; *J. Phys. D: Appl. Phys.*, **2002**, *35*, 2206. **DOI:** 10.1088/0022-3727/35/17/318
29. Kargirwar, S.; Thakare, S.; Choudhary, M.; Kondawar, S.; Dhakate, S.; *Adv. Mat. Lett.*, **2011**, *2*, 397**.** **DOI:** 10.5185/amlett.2011.4245
30. Zuo, F.; Angelopoulos, M.; MacDiarmid A.; Epstein, A.; *Phys. Rev. B.*, **1987**, *36*, 3475. **DOI:** 10.1103/PhysRevB.36.3475
31. Kobayashi, A.; Ishikawa, H.; Amano K.; Satoh, M.; *J. Appl. Phys.*, **1993**, *74*, 296. **DOI:** 10.1063/1.354106
32. More, P.; Khollam, Y.; Deshpande, S.; Sainkar, S.; Date, S.; Karekar R.; Aiyer, R.; *Mater. Lett.*, **2003**, *57*, 2177. **DOI:** 10.1016/S0167-577X(02)01170-9
33. More, P.; Khollam, Y.; Deshpande, S.; Sainkar, S.; Date, S.; Karekar, R.; Aiyer, R.; *Mater. Lett.*, **2003**, 8, 205. **DOI:** 10.1016/S0167-577X(03)00446-4
34. Lantoo V.; Ramppainen P.; *J. Electrochem. Soc*., **1998**, *135*, 2550. **DOI:** 10.1149/1.2095378